

Macular and Plasma Xanthophylls Are Higher in Age-related Macular Degeneration than in Normal Aging

Alabama Study on Early Age-related Macular Degeneration 2 Baseline

Gerald McGwin, Jr., PhD,^{1,2} Deepayan Kar, MS,¹ Andreas Berlin, MD,^{1,3} Mark E. Clark, MEng,¹ Thomas A. Swain, MPH,^{1,2} Jason N. Crosson, MD,^{1,4} Kenneth R. Sloan, PhD,^{1,5} Cynthia Owsley, PhD, MSPH,¹ Christine A. Curcio, PhD¹

Purpose: Quantification of retinal xanthophyll carotenoids in eyes with and without age-related macular degeneration (AMD) via macular pigment optical volume (MPOV), a metric for xanthophyll abundance from dual wavelength autofluorescence, plus correlations to plasma levels, could clarify the role of lutein (L) and zeaxanthin (Z) in health, AMD progression, and supplementation strategies.

Design: Cross-sectional observational study (NCT04112667).

Participants: Adults ≥ 60 years from a comprehensive ophthalmology clinic, with healthy maculas or maculas meeting fundus criteria for early or intermediate AMD.

Methods: Macular health and supplement use was assessed by the Age-related Eye Disease Study (AREDS) 9-step scale and self-report, respectively. Macular pigment optical volume was measured from dual wavelength autofluorescence emissions (Spectralis, Heidelberg Engineering). Non-fasting blood draws were assayed for L and Z using high-performance liquid chromatography. Associations among plasma xanthophylls and MPOV were assessed adjusting for age.

Main Outcome Measures: Age-related macular degeneration presence and severity, MPOV in fovea-centered regions of radius 2.0° and 9.0°; plasma L and Z ($\mu\text{M}/\text{ml}$).

Results: Of 809 eyes from 434 persons (89% aged 60–79, 61% female), 53.3% eyes were normal, 28.2% early AMD, and 18.5% intermediate AMD. Macular pigment optical volume 2° and 9° were similar in phakic and pseudophakic eyes, which were combined for analysis. Macular pigment optical volume 2° and 9° and plasma L and Z were higher in early AMD than normal and higher still in intermediate AMD ($P < 0.0001$). For all participants, higher plasma L was correlated with higher MPOV 2° (Spearman correlation coefficient [R_s] = 0.49; $P < 0.0001$). These correlations were significant ($P < 0.0001$) but lower in normal ($R_s = 0.37$) than early and intermediate AMD ($R_s = 0.52$ and 0.51, respectively). Results were similar for MPOV 9°. Plasma Z, MPOV 2°, and MPOV 9° followed this same pattern of associations. Associations were not affected by supplement use or smoking status.

Conclusions: A moderate positive correlation of MPOV with plasma L and Z comports with regulated xanthophyll bioavailability and a hypothesized role for xanthophyll transfer in soft drusen biology. An assumption that xanthophylls are low in AMD retina underlies supplementation strategies to reduce progression risk, which our data do not support. Whether higher xanthophyll levels in AMD are due to supplement use cannot be determined in this study. *Ophthalmology Science* 2023;3:100263 © 2022 by the American Academy of Ophthalmology. This is an open access article under the CC BY-NC-ND license (<http://creativecommons.org/licenses/by-nc-nd/4.0/>).



Supplemental material available at www.ophtalmologyscience.org.

Age-related macular degeneration (AMD) is a globally prevalent disease of aging that is managed medically in the 15% of patients with exudative complications. An underlying degeneration affects the photoreceptor support system

of choriocapillary microvasculature, Bruch's membrane (BrM), and retinal pigment epithelium (RPE), in the setting of extracellular deposits that mirror the spatial distributions of cones and rods.¹ Initial trial results for inhibitors of

complement pathway components,^{2,3} the largest implicated by genetics, show promise in slowing the expansion of atrophy. Targeted treatments at earlier stages of disease, before irreversible tissue damage and vision loss, are a research priority.

The macular pigment (MP) comprises 2 polar xanthophyll carotenoids of dietary origin [3R, 3'R, 6'R]-lutein (L) and [3R, 3'R]-zeaxanthin (Z), plus an intraocularly produced metabolite [3R, 3'S; meso]-Z. All are concentrated in the 3-mm diameter macula lutea, with Z highest in the foveal central bouquet.^{4,5} A secondary analysis of the Age-related Eye Disease Study 2 (AREDS2) showed lower risk for neovascularization in patients with large drusen consuming oral supplements with L, Z, and vitamins.⁶ The trial hypothesized that MP improves retinal membrane stability, filters short-wavelength light, and maintains intra- and extracellular redox balance, among other mechanisms.^{4,7} No specific AMD pathology was mentioned. Xanthophyll transfer from foods and supplements to target tissue (bioavailability) depends on processes including digestion, absorption, transport, and uptake by and stabilization within retinal cells.⁸ New data along this xanthophyll bioavailability axis are relevant to the AREDS2 mechanism of action, potentially leading to improved public health messaging and novel interventions.

Dual wavelength autofluorescence imaging can detect retinal xanthophyll abundance in vivo (Fig S1), thus elucidating 1 step of bioavailability. Macular pigment in a fundus projection plane is macular pigment optical density (MPOD). Macular pigment optical density integrated over the central area is macular pigment optical volume (MPOV).^{9,10} This imaging modality is based on the strong emission signal elicited from RPE lipofuscin by blue (488 nm) and green (514 nm) excitation lights. Intensities at fixation, where blue light is blocked by MP, are compared to intensities at an eccentric reference point where MPOD is near 0. Relative to psychophysical tests involving color matching (heterochromatic flicker photometry),¹¹ dual wavelength autofluorescence imaging is quick, objective, repeatable, and comprehensive, i.e., all pixels are available for analysis. Our previous study using this technique¹² showed that MPOV was higher in early AMD than in normal eyes, and higher still in intermediate AMD eyes. Although 64% of study participants with intermediate AMD reported supplement use, higher MPOV could not be attributed to supplement use, due to the small size of the study (N = 88 total, 33 intermediate AMD).

A recent conceptual advance is the linkage of xanthophylls and the biogenesis of soft drusen. These deposits directly precede type 1 macular neovascularization^{13–15} and atrophy,¹⁶ constitute the highest population-level ocular risk factor for AMD progression,^{17,18} and cluster under the central macula. This high-risk drusen area matches the horizontal extent in the retinal plexiform layers of the Müller glia,¹⁸ now recognized as major xanthophyll reservoirs.^{19–25} Longitudinal clinical imaging and laboratory studies together suggest that drusen form due to impaired transport of material normally released from RPE

to circulation across aged BrM and choriocapillaris.^{26–29} Drusen are preceded by age-related lipid accumulation in BrM, the composition of which indicates a dietary source for fatty acids.^{30,31} Further, RPE cell lines take up xanthophylls carried by plasma low density lipoprotein and high density lipoprotein (HDL)³² and transfer them to neurosensory retina via carrier proteins.³³ Lutein and Z may serve to facilitate neural efficiency for foveal cone vision,³⁴ in addition to accepted roles in retinal optics and antioxidant neuroprotection.

The mechanism of action of oral supplements containing L and Z would benefit from new data on tissue level MP concentration and plasma levels of carotenoids, at early stages of AMD, interpreted in the context of deposit-driven disease. The current cross-sectional study measured MPOV and plasma carotenoids in participants whose eyes were graded for AMD presence and severity using the AREDS 9-step scale for color fundus photography.

Methods

Regulatory Approval

This study was approved by the Institutional Review Board of the University of Alabama at Birmingham. All participants provided written informed consent after the nature and purpose of the study were explained. Conduct of the study followed the tenets of the Declaration of Helsinki.

Participants

Baseline data from the Alabama Study on Early Age-related Macular Degeneration 2 (ALSTAR2) are used in this analysis. The ALSTAR2 is a prospective cohort study on normal aging and early and intermediate AMD whose purpose is to validate visual function testing with retinal imaging characteristics in these conditions (Clinicaltrials.gov identifier NCT04112667, October 7, 2019).³⁵

Participants ≥ 60 years old were recruited from the Callahan Eye Hospital Clinics, the clinical service of the University of Alabama at Birmingham Department of Ophthalmology and Visual Sciences. We filled 3 participant groups—persons with early AMD and intermediate AMD and those in normal macular health. The clinic's electronic health record was used to search for patients with early or intermediate AMD using International Classification of Diseases 10 codes for these conditions (H35.30*; H35.31*; H35.36*). An author (C.O.) screened charts to ensure that participants met the eligibility criteria. Exclusion criteria were (1) any eye condition or disease in either eye (other than early cataract) in the medical record that can impair vision including diabetic retinopathy, glaucoma, ocular hypertension, history of retinal diseases (e.g., retinal vein occlusion, retinal degeneration), optic neuritis, corneal disease, previous ocular trauma or surgery, refractive error ≥ 6 diopters; (2) neurological conditions that can impair vision or judgment including multiple sclerosis, Parkinson's disease, stroke, Alzheimer's disease, seizure disorders, brain tumor, traumatic brain injury; (3) psychiatric disorders that could impair the ability to follow directions, answer questions about health and functioning, or to provide informed consent; (4) diabetes; (5) any medical condition that causes liver disease, significant frailty or was thought to be terminal. Persons in normal macular health were recruited with the same eligibility criteria except they did not have International Classification of Diseases 10 codes indicative of

AMD. Letters were sent to potential participants, and the study coordinator followed up with a phone call to determine interest.

Classification into the 3 groups was based on a trained grader's (M.E.C.) evaluation of 3-field, color fundus photographs taken with a digital camera (450+, Carl Zeiss Meditec) following dilation with 1% tropicamide and 2.5% phenylephrine hydrochloride. The AREDS 9-step classification system³⁶ was used by a trained grader (M.E.C.) to identify AMD presence and severity in each eye and assign into groups. Groups were defined as follows: those eyes with normal macular health had AREDS grade 1, early AMD had grades 2 to 4, and intermediate AMD had grades 5 to 8. The grader was masked to all other participant characteristics.

Demographic and health-related characteristics (age, sex, race/ethnicity, oral carotenoid supplement use, smoking status) were obtained through participant interview. Lens status was determined by anterior segment slit lamp photographs (Carl Zeiss Meditec 450+).

Carotenoid Assays

Details are available in the [Supplementary Methods](#). In brief, plasma L and Z were determined in non-fasting blood draws at Eurofins Craft. Individual carotenoids were measured by high-pressure liquid chromatography in plasma that had been stored at -70°C using a modification of previously described procedures.^{37,38} Plasma protein and lipoproteins were denatured with ethanol. Once denatured lipid soluble substances were extracted into hexane and separated by reverse phase liquid chromatography based on their lipophilicity. Carotenoids are detected at 450 nm visible range. The calibration method is based on external standards using peak areas and corrected for tocol as the internal standard.

Imaging Acquisition and Analysis for Macular Xanthophyll Pigment

Detailed imaging protocols based on our previous study¹² are found in the [Supplementary Methods](#) and are briefly described here. Multimodal imaging included near infrared reflectance and spectral-domain OCT; 8.6×7.2 mm ($30^{\circ} \times 25^{\circ}$ field, 121 scans) horizontal macular volume centered on the fovea.

Dual wavelength autofluorescence for MPOD and MPOV ([Fig S1](#)) can be distinguished from other imaging methods for xanthophyll assessment with similar names including dual wavelength autofluorescence fluorometry,³⁹ single wavelength autofluorescence,⁴⁰ dual wavelength reflectance,⁴¹ single wavelength reflectance,⁴² and fluorescence lifetime ophthalmoscopy.⁴³ The Spectralis investigational MPOD module uses confocal scanning laser ophthalmoscopy with blue ($\lambda = 488$ nm) and green ($\lambda = 514$ nm) laser diodes for autofluorescence excitation. As described,¹⁰ MPOD is the \log_{10} of the ratio of green-excited autofluorescence intensities to blue-excited autofluorescence intensities emitted by the RPE, calculated at each pixel location. Macular pigment optical density data were exported from the Spectralis and processed by custom FIJI plugins (<https://www.nature.com/articles/nmeth.2019>) (ImageJ v1.52; National Institutes of Health [NIH]⁴⁴; [Supplementary Methods](#)). Autofluorescence imaging sessions were reviewed for quality. Images that were not evenly illuminated, well focused, or had evidence of floaters or other obscuration were excluded.

We computed MPOV as mean MPOD \times mm² for disks centered on the fovea with radius of 2.0° (0.58 mm) and 9.0° (2.56 mm). Macular pigment optical density values were normalized by setting the mean MPOD value at eccentricity 9.0° to 0. For comparison to horizontally oriented OCT B-scans through the fovea,

Table 1. Demographic Characteristics of Participants (N = 434)

| Variable names and groups | Mean (SD) or n (%) |
|----------------------------------|--------------------|
| Age (years) | 71.8 (6.1) |
| Age group | |
| 60–69 | 152 (35.0) |
| 70–79 | 236 (54.4) |
| 80–89 | 44 (10.1) |
| 90–99 | 2 (0.5) |
| Gender | |
| Male | 170 (39.2) |
| Female | 264 (60.8) |
| Race | |
| White | 391 (90.1) |
| Black | 36 (8.3) |
| Other* | 7 (1.6) |
| Smoking | |
| Ever (current/past) | 179 (41.2) |
| Never | 255 (58.8) |
| Oral supplement use [†] | |
| Yes | 88 (20.3) |
| No | 346 (79.7) |

SD = standard deviation.

*Other includes 4 Asians or Pacific Islanders and 3 Native Americans.

[†]Self-reported supplementation with lutein and/or zeaxanthin such as Preservision/ Age-related Eye Disease Study (AREDS), Lutigold, Provision, Macular Health, Adult 50+ Eye Health, OcuVite.

we determined MPOD as the mean intensity of all pixels at each eccentricity, within two 30° -wide wedges with the tips at the fovea and aligned on the horizontal meridian.

Statistical Analysis

Only those eyes meeting image quality criteria (see above) in individuals with plasma xanthophyll measurements were used. Macular pigment optical volume was compared between eyes with natural and artificial lenses. Macular pigment optical volume and xanthophyll measurements were compared with respect to AMD severity categorized as normal, early, and intermediate using linear mixed models. Spearman correlation coefficients (R_s) were estimated for the association between MPOV and xanthophyll measurements both overall and according to AMD severity and supplementation use. Effect modification by ever/never smoker was assessed. The level of significance was 0.05 (2-sided). All analyses were completed using SAS (version 9.4, SAS Institute).

Results

[Table 1](#) shows the characteristics of the study participants. Of 434 individuals, 60.8% were women, 90.1% were white, and 41.2% were current or former smokers. Of this sample, 88 individuals (20.3%) reported use of oral carotenoid supplements. A flowchart for selecting 809 eyes for MPOV analysis is shown in [Fig S2](#).

Aged natural lenses and artificial lenses potentially affect the blue component of MPOV in different ways. In phakic eyes, opacification and autofluorescence of the aged lens together add noise to measurements of blue emission autofluorescence. Further, in some pseudophakic eyes, the implanted lenses may also reduce blue light transmission.

Table 2. Lens Status, Macular Pigment Optical Volume, and Plasma Xanthophylls: All Eyes and Stratified by Age-related Eye Disease Study 9-step AMD Status and Severity

| | All Eyes N = 809 | Normal N = 431 (53.3%) | Early AMD N = 228 (28.2%) | Intermediate AMD N = 150 (18.5%) | P Values |
|---|---------------------|---------------------------|------------------------------|----------------------------------|----------|
| Lens status, N (%) | | | | | |
| Phakic | 428 (52.9) | 256 (52.9) | 112 (49.1) | 60 (40.0) | |
| Pseudophakic | 381 (47.1) | 175 (40.6) | 116 (50.9) | 90 (60.0) | |
| MPOV 2.0°, mean (SD) | 0.36 (0.15) | 0.33 (0.13) | 0.36 (0.14) | 0.44 (0.17) | < 0.0001 |
| MPOV 9.0°, mean (SD) | 1.43 (0.61) | 1.34 (0.50) | 1.46 (0.64) | 1.67 (0.77) | < 0.0001 |
| Lutein, mean $\mu\text{M}/\text{ml}$ (SD) | 0.44 (0.40) | 0.35 (0.25) | 0.49 (0.52) | 0.64 (0.45) | < 0.0001 |
| Zeaxanthin, mean $\mu\text{M}/\text{ml}$ (SD) | 0.14 (0.09) | 0.13 (0.08) | 0.14 (0.09) | 0.19 (0.12) | < 0.0001 |

AMD = age-related macular degeneration; MPOV = macular pigment optical volume; SD = standard deviation.

Of 431, 228, and 150 eyes in normal, early AMD, and intermediate AMD groups, 24 (15.2%), 52 (22.8%) and 82 (54.7%) came from persons reporting supplement use.

Obana et al demonstrated that signal was 10% to 15% higher after cataract surgery than before surgery and derived a one-size-fits-all correction factor for age.^{45,46} Fig S3 shows that MPOV 2° and 9° in phakic and pseudophakic eyes in our sample followed similar trends and did not significantly differ. Thus, we combined both phakic and pseudophakic eyes into a single sample and adjusted the statistical model for binocular data.

Table 2 compares MPOV (2° and 9°) and plasma L and Z per AMD status, indicating a statistically significant increase in the values of each measure with increasing AMD severity. For all eyes, the correlation between plasma L and MPOV 2° was 0.49 ($P < 0.0001$) (Table 3). These correlations were all significant ($P < 0.0001$) but lower in normal ($R_s = 0.37$) than early and intermediate AMD ($R_s = 0.52$ and 0.51 , respectively). The pattern of correlations was similar for MPOV 9°. With respect to plasma Z, for all eyes the correlation with MPOV 2° was $R_s = 0.43$ ($P < 0.0001$) and was weaker for normal eyes ($R_s = 0.21$) than for eyes with early and intermediate AMD (both $R_s = 0.46$). As with L, this pattern of correlations was consistent for MPOV 9°. The aforementioned correlations did not differ according to self-reported supplement use (Table S4), except for normal eyes, which become non-significant. Correlations also did not differ according to smoking status (results not shown).

Figure 4 shows representative structural OCT and dual wavelength autofluorescence imaging of MPOD in a normal eye and eyes with early and intermediate AMD. All 3 eyes have a central area of peak signal reducing with foveal eccentricity. The spatial distribution of macular pigment is slightly elongated in the horizontal direction. In an older normal eye (Fig 4A), OCT B-scan shows uniform and regular outer retinal hyperreflective bands. The *en face* MPOD distribution exhibits a central peak surrounded by a secondary ring centered around the foveal center. Macular pigment optical density profiles showed corresponding central peak shouldered by sub-peaks of lower densities. Macular pigment optical density reaches near-zero at 9° eccentricity. An early AMD eye (B) has drusen in the parafoveal region (magnified in inset). A sharp central MPOD peak surrounded by a weak elliptical *en face* MPOD distribution is seen. An eye with intermediate AMD (Fig 4C) has multiple drusen in the parafovea and higher central peak of MPOD compared with the normal and early AMD cases, with patterned spots of deeper signal loss related to drusen. In addition to elevated peak MPOD levels with AMD severity, representative cases show the variation of MPOD shape.

Figure 5 shows mean MPOD profiles along the horizontal meridian for all study eyes, computed as described in the Methods, and stratified by diagnostic

Table 3. Spearman Correlations of MPOV 2.0°, MPOV 9.0°, Lutein, and Zeaxanthin in All Eyes and by Age-related Eye Disease Study 9-step AMD Status and Severity

| | Lutein | | | | Zeaxanthin | | | |
|------------------|-----------|----------|-----------|----------|------------|----------|-----------|----------|
| | MPOV 2.0° | | MPOV 9.0° | | MPOV 2.0° | | MPOV 9.0° | |
| | R_s | P Value | R_s | P Value | R_s | P Value | R_s | P Value |
| All eyes | 0.49 | < 0.0001 | 0.54 | < 0.0001 | 0.43 | < 0.0001 | 0.43 | < 0.0001 |
| Normal | 0.37 | < 0.0001 | 0.47 | < 0.0001 | 0.21 | < 0.0001 | 0.31 | < 0.0001 |
| Early AMD | 0.52 | < 0.0001 | 0.59 | < 0.0001 | 0.46 | < 0.0001 | 0.53 | < 0.0001 |
| Intermediate AMD | 0.51 | < 0.0001 | 0.53 | < 0.0001 | 0.46 | < 0.0001 | 0.49 | < 0.0001 |

AMD = age-related macular degeneration; MPOV = macular pigment optical volume; R_s = Spearman correlation coefficient.

group. The differences among groups are small, and intermediate AMD is clearly higher than the others.

Discussion

Our main finding is a moderately high positive correlation between MPOV and plasma xanthophyll that did not differ by AMD status. We also observed higher levels of MPOV in AMD eyes compared to normal eyes also, consistent with our previous report¹² using similar methods on a smaller sample from the same clinic. Higher supplement use in participants with AMD cannot be confirmed as an explanation for the latter finding due to our study design, as

elaborated below. Importantly, higher retinal and plasma xanthophylls in AMD occurred in persons not reporting supplement use (Table S1). We interpret our results in the context of a xanthophyll bioavailability axis and a model of how xanthophyll transfer could contribute to drusen formation.

Across the entire cohort, we found that both MPOV 9° and 2° correlated moderately ($R_s = 0.5$) to plasma L measures, with lower measures for normal eyes ($R_s = 0.37$). A similar pattern of correlations, at lower levels, was found for Z (R_s range 0.43–0.53 for AMD and $R_s = 0.31$ for normal). The relationship between plasma and tissue levels has been long investigated using psychophysical and imaging measures of MP, as summarized for 22 studies including ours in Table S5. Our correlation coefficients using comprehensive

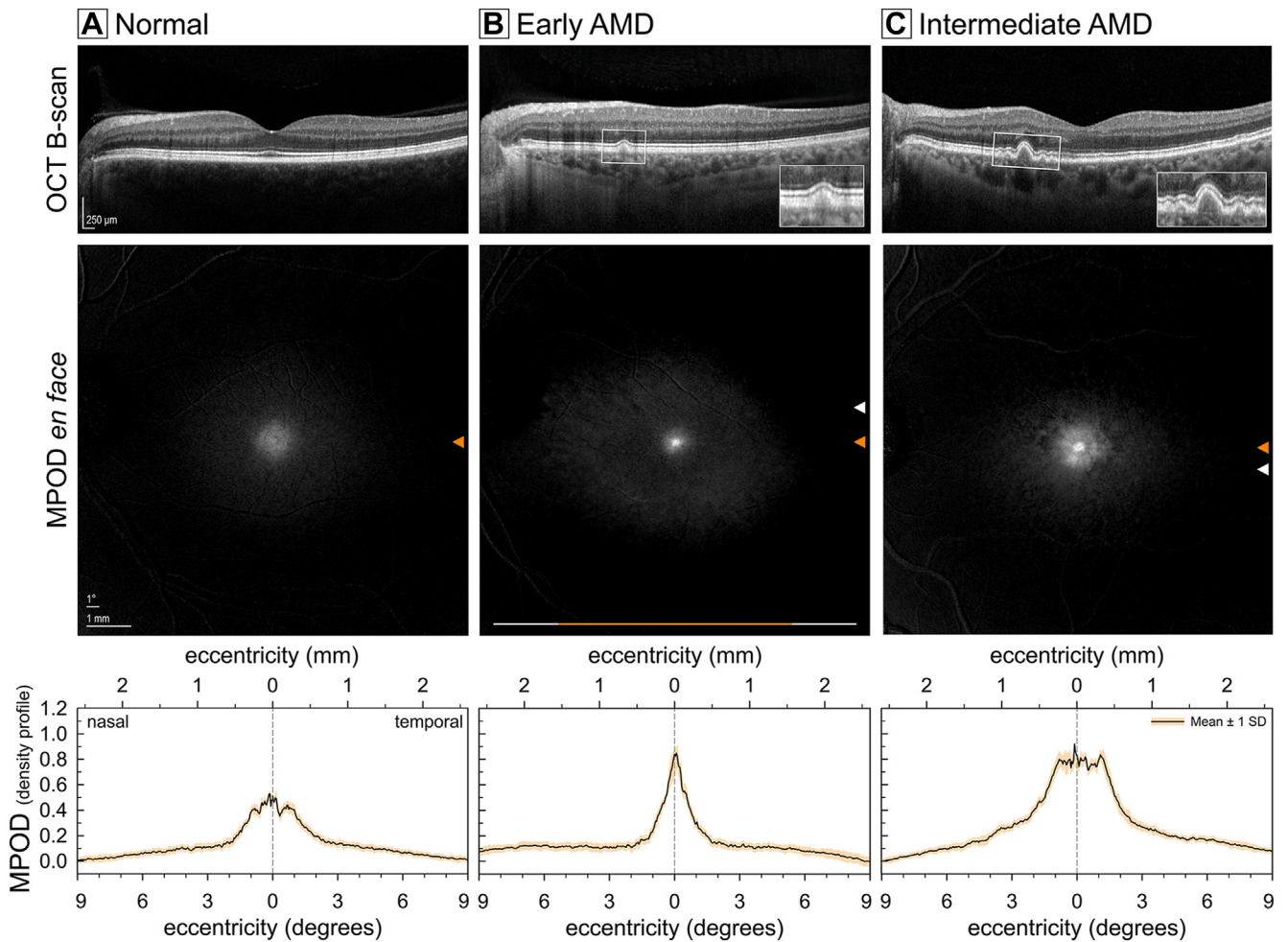


Figure 4. Structural and macular xanthophyll pigment imaging in eyes with and without early and intermediate age-related macular degeneration (AMD). Comparison of foveal OCT B-scans (top row), spatial distribution of xanthophyll carotenoids using dual-wavelength autofluorescence (middle row), and density distribution profile of macular pigment optical density (MPOD) (bottom row) in representative cases near the mean macular pigment optical volume (MPOV) for each diagnostic group (Age-related Eye Disease Study [AREDS] stages indicated). Full extent of the line in the middle panel represents the extent of the 30° OCT B-scan. Orange scale bar overlay represents the extent of 18° MPOD density sampled from two 30°-wide wedges centered on the fovea (resembling a bowtie). Orange arrowheads represent the horizontal meridian for the MPOD plots. White arrowheads represent y-locations of sampled B-scans. Scale bar (top panels) = 250 μ m. OCT B-scans in top row show a healthy macula (A) and soft drusen with intact outer retinal bands in (B, C). We used a universal conversion of 0.288 mm/° of visual angle. Two-wavelength autofluorescence imaging for intermediate AMD shows decreased signal corresponding to the drusen. Representative cases show the variation in MPOD shape as well as the higher MPOV in early and intermediate AMD relative to normal eyes. Graphs were plotted using RStudio (Integrated Development for R) and Excel (version 16.64 for Mac, Microsoft).

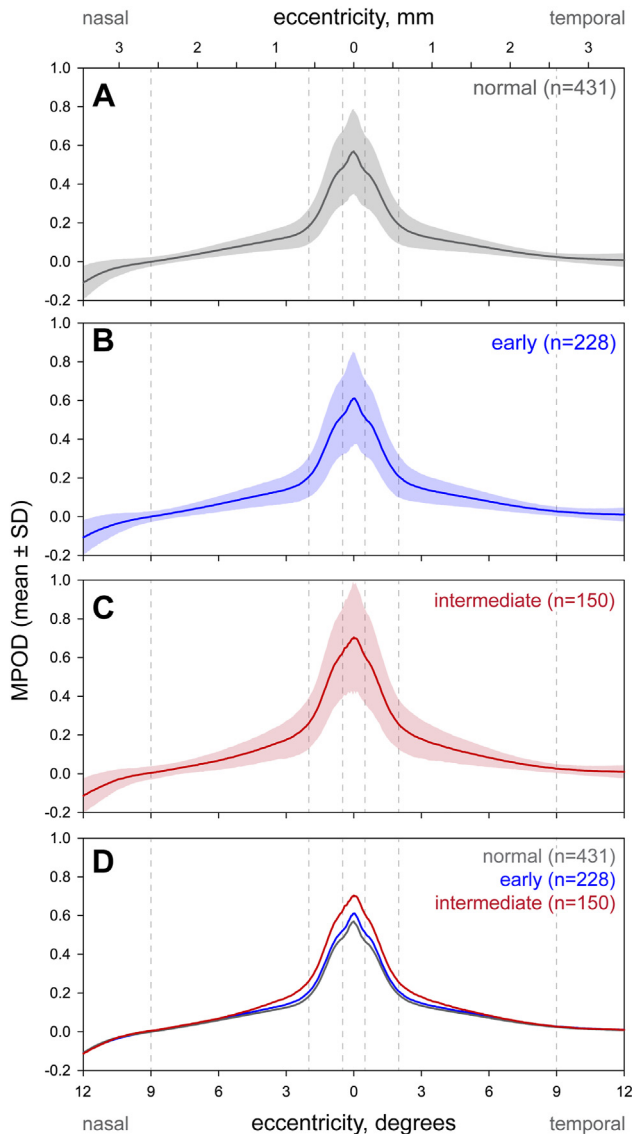


Figure 5. Macular xanthophyll pigment density distribution in eyes with and without early and intermediate age-related macular degeneration (AMD). **A, B, C,** Mean (line) and standard deviation colored band of 12° macular pigment optical density (MPOD) profiles sampled from 2 wedges (resembling a bowtie) and plotted as a function of foveal eccentricity generated from 431 normal, 228 early, and 150 intermediate AMD eyes. **D,** Mean MPOD density profiles for the respective groups. A conversion factor of 0.288 mm/° of visual angle is used. SD = standard deviation.

imaging and analysis are among the highest reported to date. Prior analyses also resulting in strong correlations used point estimates of MPOD (0.73 at 1°, n = 59⁴⁷; 0.61 at 0.5°, n = 88⁴⁸; 0.61 at 0.5°, n = 88⁹). In a study similar to ours (Montrachet),⁴⁹ 433 older adults were imaged by dual wavelength autofluorescence and stratified by AMD fundus. Correlations between MPOD (0.5° and average within 0.5° radius) and plasma L and Z were significant at a much lower R_s (0.10) than ours. The ALSTAR2 and Montrachet differed in patient population, image quality controls, and MP metrics. Because of the many technical

and cohort differences among the studies in Table S5, the significance of our current findings for AMD progression will best be determined with the 3-year follow-up visit for ALSTAR2.

Both MPOV 9° and MPOV 2° were highest in intermediate AMD eyes.¹² One reason why L and Z were proposed as protective for AMD is that early studies suggested that person-level AMD risk factors like smoking and female sex were also associated with low MP measured by heterochromatic flicker photometry.^{50–52} An assumption of low retinal MP in AMD underlies the rationale for oral supplements containing L and Z. This assumption has been difficult to test in vivo, in part because assays of MP abundance did not account well for the cellular composition, geometry, and population-level variability in foveal structure.⁵³ This variability in turn results from differences in the rate, timing, and extent of complex cellular interactions in foveal development, involving prenatal creation of a pit and postnatal squeezing together of cones.^{54,55} In the adult fovea, cones are densely packed,⁵⁶ with a 10-fold decline in all directions within 1 mm (3.5°) eccentricity. Müller glia may be equally numerous.⁵⁷ Rings, crests, plateaus, and other manifestations of either an absent peak or a non-monotonic decline have been noted in up to 40% of study participants,^{40,58–62} regardless of detection technology, including ours (Fig 4). Many prior studies using both heterochromatic flicker photometry and dual wavelength autofluorescence reported single values for MPOD at 0.5° (~144 μm eccentricity), i.e., only partly including the Z-rich central bouquet.^{23,25} Authors of a supplementation study noted that detecting a treatment effect depended on how the foveal center was defined.⁶³ Commercially available and prototype imaging technology currently defines the foveal center in several ways,^{64–66} each having distributions that may be offset from each other.⁶⁷ Macular pigment optical volume 2° in our studies captures the central 1.15 mm diameter of macula and does not assess smaller anatomical features within that region.⁶⁰ Our future studies of MPOD and MPOV variability will account for structural details by linking dual wavelength autofluorescence with OCT.⁶²

We interpret our results within the framework of a regulated axis of carotenoid bioavailability from gut to retina.^{32,68,69} Carotenoids are 40-carbon organic pigments synthesized in plants, bacteria, and fungi. Hydrocarbon forms of carotenoids are termed carotenes while oxygenated forms are termed xanthophylls. Six major carotenoids in human plasma include α-carotene, β-carotene, β-cryptoxanthin, L, Z, and lycopene. Some are metabolically converted to vitamin A or retinol. Major xanthophylls lacking provitamin A activity include L and Z. Mechanisms of micronutrient absorption, distribution, metabolism, and excretion are under investigation and involve microbiota, uptake into and efflux out of intestinal epithelium, secretion of chylomicrons into the lymphatics, transport in plasma via lipoproteins, deposition in target tissues via receptors and transporters, storage, and catabolism. Genetic variance in these enzymes and transporters (nutrigenetics) thus likely affect xanthophyll distribution in the macula lutea.^{52,70} As

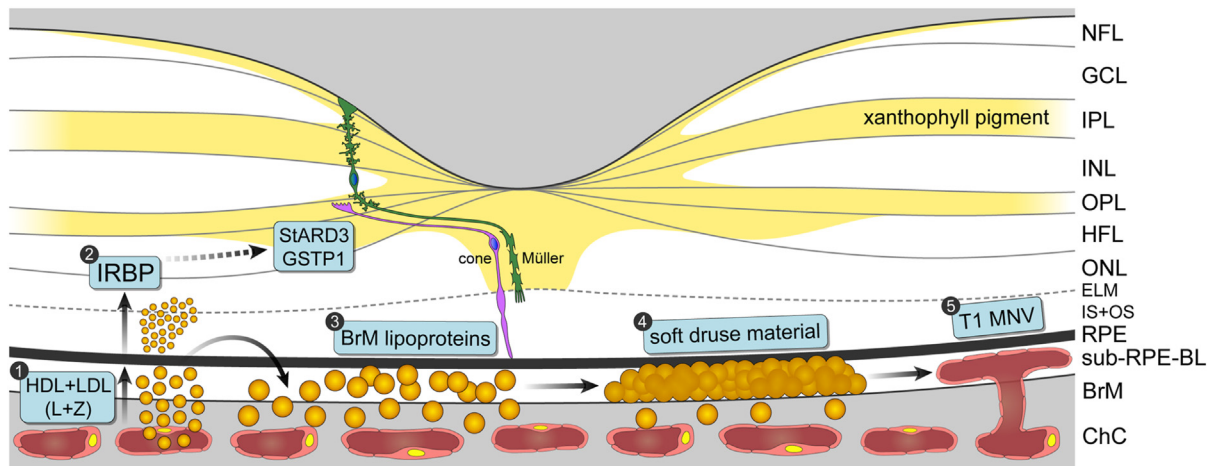


Figure 6. Hypothesis: xanthophyll transfer, soft drusen biogenesis, and type 1 macular neovascularization (T1 MNV). Schematized xanthophyll localization is adapted¹² from microdensitometry of monkey retinal tissue sections.²³ Five steps are depicted. 1. Plasma high density lipoprotein (HDL) and low density lipoprotein (LDL) carrying lutein (L) and zeaxanthin (Z)⁷² are taken up at retinal pigment epithelium (RPE) receptors (scavenger receptor B-1 and LDL receptor).⁸¹ 2. RPE extracts xanthophylls for transfer to retina via interphotoreceptor retinal binding protein (IRBP)³³ and possibly others.⁸² Cellular xanthophyll binding proteins glutathione S-transferase 1 (GSTP1) and steroidogenic acute regulatory protein-related lipid transfer domain 3 (StARD3) have been localized in cones.^{83,84} Xanthophylls have been localized in retinal layers beyond those accounted for by cones and in places consistent with Müller glia, suggesting additional proteins with binding and transfer capability such as fatty acid binding protein 5.⁸⁵ 3. RPE constitutively releases unneeded lipids back to circulation in large lipoproteins containing apolipoproteins B and E. 4. Lipoprotein particles accumulate in Bruch's membrane (BrM) starting in late adolescence and build up through adulthood⁸⁶ due to impaired transport across aging BrM (which becomes cross-linked) and choriocapillaris (ChC) endothelium (which degenerates). These accumulate as soft drusen material, separating RPE from ChC and containing proinflammatory, proangiogenic peroxidized lipids in an atherosclerosis-like progression.^{87,88} 5. Soft drusen material is a direct precursor of type 1 (choroid-originating) neovascularization.^{13,14} ELM = external limiting membrane; GCL = ganglion cell layer; HFL = Henle fiber layer; INL = inner nuclear layer; IPL = inner plexiform layer; IS = inner segments; NFL = nerve fiber layer; ONL, outer nuclear layer; OPL = outer plexiform layer; OS = outer segments; sub-RPE-BL = sub-RPE-basal lamina.

explored in classic twin studies of largely White women,^{63,71} heritability was high (0.67–0.85) for the distribution of MPOD. Further, 27% of the response to L and Z supplementation in 161 twin pairs was accounted for by genetic factors.⁸ Scavenger receptor BI is a multiligand cell surface receptor that mediates selective uptake of HDL, a major xanthophyll carrier⁷² in liver and in RPE⁷³; single nucleotide polymorphism rs11057841 of *SCARB1* gene is associated with higher MPOD.⁷⁴ Regulation of xanthophyll bioavailability is a strong candidate pathway for the AMD HDL genes (apolipoprotein E, cholesteryl ester transfer protein, ATP binding cassette subfamily A member 1), which are expressed within the eye^{75,76} as well as systemically.

This and our prior study collectively cannot address the merits of L and Z supplementation, currently recommended to reduce progression risk, due to cross-sectional design. Further, the number of supplement users was small, supplement formulations were variable, and adherence was not measured. Nevertheless, our finding that MPOV 2° and 9° are highest in intermediate AMD eyes, in the setting of higher plasma L and Z in the same persons, is relevant to the rationale for supplementation. Supplementation strategies in general assume that AMD eyes have low xanthophyll concentration in neurosensory retina, which our current data may not support. We caution that important aspects of the bioavailability axis and the potential impact of L and Z are not captured by MPOV. For example, in a small L

supplementation trial (n = 72), Berendschot et al demonstrated modulation of systemic complement factors and, by inference, systemic inflammation.^{77,78} Others suggested that rather than native xanthophylls, metabolites may be the active agents. For example, carotenoids in a prooxidant environment can convert to cytotoxic aldehydes⁷⁹ or generate cleavage products that interact with nuclear receptors regulating proinflammatory transcription factors.⁶⁹ In these situations, additional L or Z may overwhelm downstream enzymes and be harmful. However, the AREDS2 trial did show in a secondary analysis that L and Z reduced neovascular AMD in a very large sample (n = 4203 eyes) over 5 years and persisted to 10 years, without evidence for a survivor bias.⁸⁰

In Figure 6 we offer a new hypothesis for the role of L and Z in retinal health and AMD, invoking bioavailability components of retinal uptake, transfer, and elimination, and aspects of AMD pathophysiology not considered in previous inquiries, including AREDS2. We focus on the tight foveal concentration of high-risk soft drusen under the macula lutea and the well-documented progression of soft drusen to type 1 (choroid-originating) neovascularization.^{13,14} Plasma HDL and low density lipoprotein carrying L and Z are taken up at RPE receptors. Retinal pigment epithelium extracts xanthophylls for transfer to retina. Cellular xanthophyll binding proteins have been localized in cones. Xanthophylls have also been localized in Müller glia, suggesting involvement of additional

proteins. Retinal pigment epithelium constitutively releases unneeded lipids back to circulation in large lipoproteins containing apolipoproteins B and E. Lipoprotein particles accumulate in BrM starting in late adolescence and build up through adulthood due to impaired transport across aging BrM and choriocapillaris endothelium. Lipoproteins accumulate as soft drusen material, containing proinflammatory, proangiogenic peroxidized lipids. Separating RPE from choriocapillaris leads to upregulated VEGF secretion and onset of type 1 neovascularization. We previously proposed that foveal shape and thickness may focus the vertical component of lipid transfer and thus modulate the horizontal extent of sub-RPE lipoprotein accumulation.¹² In the model in Figure 6, supplementation with L and Z potentially enriches HDL and low density lipoprotein, suppressing uptake by RPE, resulting in fewer large lipoproteins released into BrM, reduced drusen volume, and reduced risk for type 1 neovascularization.

Strengths of our study include a large sample including many normal eyes at the aging-AMD interface, an objective imaging method for MP, high quality images, plasma carotenoid measures on 90% of participants, and standardized fundus grading. Limitations include a study designed for structure-function relationships rather than xanthophyll biology, a cross-sectional sample, and an imaging device

that is not yet widely available. Xanthophyll distribution and transfer figures prominently in the Center-Surround model of foveal cone resilience and parafoveal rod vulnerability underlying the investigation of vision and imaging indicators in ALSTAR2.^{89,90} Future analyses will examine morphologic, metabolic, and genetic determinants of individual variability in MP distribution, and how MP affects visual function. At 3-year follow-up we can address the critical question of whether any aspect of MPOV modulates risk for progression along early stages of AMD, which would necessarily also modulate risk for advanced stages. The ALSTAR2 is not designed as a xanthophyll supplementation trial, and we do not anticipate enough conversion to neovascularization within 3 years to fully evaluate the model in Figure 6. Nevertheless, our current data generate hypotheses that can be tested in studies that are appropriately designed for those purposes.

In conclusion, MPOV assessed by dual wavelength autofluorescence was higher in early and intermediate AMD eyes than in normal eyes and positively correlated with plasma L and Z levels. Our data offer new insight into xanthophylls in retinal health and disease. Public health messaging can feature these newly appreciated benefits of xanthophylls if the model in Figure 6 is confirmed by further multidisciplinary research.

Footnotes and Disclosures

Originally received: September 10, 2022.

Final revision: November 4, 2022.

Accepted: December 16, 2022.

Available online: December 22, 2022. Manuscript no. XOPS-D-22-00191.

¹ Department of Ophthalmology and Visual Sciences, School of Medicine, University of Alabama at Birmingham, Birmingham, Alabama.

² Department of Epidemiology, School of Public Health, University of Alabama at Birmingham, Birmingham, Alabama.

³ Department of Ophthalmology, University Hospital Wurzburg, Wurzburg, Germany.

⁴ Retina Consultants of Alabama, Birmingham, Alabama.

⁵ Department of Computer Science, School of Arts and Sciences, University of Alabama at Birmingham, Birmingham, Alabama.

Disclosures:

All authors have completed and submitted the ICMJE disclosures form.

The authors have made the following disclosures: A.B.: Financial support—Dr Werner Jackstädt-foundation.

C.O.: Financial support — R01EY029595, P30EY03039, Dorsett Davis Discovery Fund, Alfreda J. Schueler Trust; Consultant — Johnson & Johnson Vision (outside this project).

C.A.C.: Financial support — R01EY029595, R01EY027948; Consultant — Boehringer Ingelheim, Apellis (outside this project); Research funds — Genentech/ Hoffman LaRoche and Regeneron.

Unrestricted funds to the Department of Ophthalmology and Visual Sciences (UAB) from Research to Prevent Blindness, Inc, and EyeSight Foundation of Alabama.

HUMAN SUBJECTS: Human Subjects were used in this study. This study was approved by the Institutional Review Board of the University of Alabama at Birmingham (UAB). All participants provided written informed

consent after the nature and purpose of the study were explained. Conduct of the study followed the tenets of the Declaration of Helsinki.

No animal subjects were used in this study.

Author Contributions:

Research design: McGwin, Kar, Berlin, Sloan, Swain, Owsley, Curcio

Data Acquisition and research execution, Kar, Berlin, Swain, Clark

Data analysis and interpretation: McGwin, Kar, Berlin, Sloan, Swain, Crosson, Owsley, Curcio

Obtained funding: Owsley, Curcio

Manuscript preparation: McGwin, Kar, Berlin, Sloan, Swain, Crosson, Owsley, Curcio

Presented at the 2022 Brain and Ocular Nutrition Conference, Cambridge, UK.

Abbreviations and Acronyms:

ALSTAR2 = Alabama Study on Early Age-related Macular Degeneration 2; **AMD** = age-related macular degeneration; **AREDS** = age-related eye disease studies; **BrM** = Bruch's membrane; **HDL** = high density lipoprotein; **L** = Lutein; **MPOD** = macular pigment optical density; **MP** = macular pigment; **MPOV** = macular pigment optical volume; **RPE** = retinal pigment epithelium; **Z** = Zeaxanthin.

Keywords:

Age-related macular degeneration, Autofluorescence, Lutein, Macular xanthophyll pigment, Zeaxanthin.

Correspondence:

Christine A. Curcio, PhD, Department of Ophthalmology and Visual Sciences, EyeSight Foundation of Alabama Vision Research Laboratories, University of Alabama at Birmingham School of Medicine, 1670 University Boulevard Room 360, Birmingham, AL 35294-0019. E-mail: christinecurcio@uabmc.edu.

References

- Chen L, Messinger JD, Kar D, et al. Biometrics, impact, and significance of basal linear deposit and subretinal drusenoid deposit in age-related macular degeneration. *Invest Ophthalmol Vis Sci.* 2021;62(1):33. <https://doi.org/10.1167/iovs.62.1.33>.
- Jaffe GJ, Westby K, Csaky KG, et al. C5 inhibitor avacincaptad pegol for geographic atrophy due to age-related macular degeneration: a randomized pivotal phase 2/3 trial. *Ophthalmology.* 2021;128:576–586.
- Liao DS, Grossi FV, El Mehdi D, et al. Complement C3 inhibitor pegcetacoplan for geographic atrophy secondary to age-related macular degeneration: a randomized phase 2 trial. *Ophthalmology.* 2020;127:186–195.
- Bernstein PS, Li B, Vachali PP, et al. Lutein, zeaxanthin, and meso-zeaxanthin: the basic and clinical science underlying carotenoid-based nutritional interventions against ocular disease. *Prog Retin Eye Res.* 2016;50:34–66.
- Polyak SL. *The Retina.* Chicago, IL: University of Chicago; 1941.
- Age-Related Eye Disease Study 2 Research Group. Lutein + zeaxanthin and omega-3 fatty acids for age-related macular degeneration: the Age-Related Eye Disease Study 2 (AREDS2) randomized clinical trial. *JAMA.* 2013;309:2005–2015.
- Krinsky NI, Landrum JT, Bone RA. Biologic mechanisms of the protective role of lutein and zeaxanthin in the eye. *Annu Rev Nutr.* 2003;23:171–201.
- Hammond CJ, Liew SH, Van Kuijk FJ, et al. The heritability of macular response to supplemental lutein and zeaxanthin: a classic twin study. *Invest Ophthalmol Vis Sci.* 2012;53:4963–4968.
- Conrady CD, Bell JP, Besch BM, et al. Correlations between macular, skin, and serum carotenoids. *Invest Ophthalmol Vis Sci.* 2017;58:3616–3627.
- Green-Gomez M, Bernstein PS, Curcio CA, et al. Standardizing the assessment of macular pigment using a dual-wavelength autofluorescence technique. *Transl Vis Sci Technol.* 2019;8:41.
- Wooten BR, Hammond Jr BR, Land RI, Snodderly DM. A practical method for measuring macular pigment optical density. *Invest Ophthalmol Vis Sci.* 1999;40:2481–2489.
- Kar D, Clark ME, Swain TA, et al. Local abundance of macular xanthophyll pigment is associated with rod- and cone-mediated vision in aging and age-related macular degeneration. *Invest Ophthalmol Vis Sci.* 2020;61:46.
- Sarks JP, Sarks SH, Killingsworth MC. Morphology of early choroidal neovascularization in age-related macular degeneration: correlation with activity. *Eye.* 1997;11:515–522.
- Chen L, Messinger JD, Kar D, et al. Biometrics, impact, and significance of basal linear deposit and subretinal drusenoid deposit in age-related macular degeneration. *Invest Ophthalmol Vis Sci.* 2021;62:33.
- Guymer RH, Rosenfeld PJ, Curcio CA, et al. Incomplete retinal pigment epithelial and outer retinal atrophy (iRORA) in age-related macular degeneration: CAM report 4. *Ophthalmology.* 2020;127:394–409.
- Chen L, Messinger JD, Ferrara D, et al. Stages of drusen-associated atrophy in age-related macular degeneration visible via histologically validated fundus autofluorescence. *Ophthalmol Retina.* 2021;5:730–742.
- Wang JJ, Rohtchina E, Lee AJ, et al. Ten-year incidence and progression of age-related maculopathy: the Blue Mountains Eye study. *Ophthalmology.* 2007;114:92–98.
- Pollreisz A, Reiter GS, Bogunovic H, et al. Topographic distribution and progression of soft drusen in age-related macular degeneration implicate neurobiology of the fovea. *Invest Ophthalmol Vis Sci.* 2021;62:26.
- Helb HM, Charbel Issa P, VAN DER Veen RL, et al. Abnormal macular pigment distribution in type 2 idiopathic macular telangiectasia. *Retina.* 2008;28:808–816.
- Powner MB, Gillies MC, Tretiach M, et al. Perifoveal Müller cell depletion in a case of macular telangiectasia type 2. *Ophthalmology.* 2010;117:2407–2416.
- Obana A, Sasano H, Okazaki S, et al. Evidence of carotenoid in surgically removed lamellar hole-associated epiretinal proliferation. *Invest Ophthalmol Vis Sci.* 2017;58:5157–5163.
- Gantner ML, Eade K, Wallace M, et al. Serine and lipid metabolism in macular disease and peripheral neuropathy. *N Engl J Med.* 2019;381:1422–1433.
- Snodderly DM, Auran JD, Delori FC. The macular pigment. II. Spatial distribution in primate retinas. *Invest Ophthalmol Vis Sci.* 1984;25:674–685.
- Trieschmann M, van Kuijk FJ, Alexander R, et al. Macular pigment in the human retina: histological evaluation of localization and distribution. *Eye (Lond).* 2008;22:132–137.
- Li B, George EW, Rognon GT, et al. Imaging lutein and zeaxanthin in the human retina with confocal resonance Raman microscopy. *Proc Natl Acad Sci U S A.* 2020;117:12352–12358.
- Balaratnasingam C, Yannuzzi LA, Curcio CA, et al. Associations between retinal pigment epithelium and drusen volume changes during the lifecycle of large drusenoid pigment epithelial detachments. *Invest Ophthalmol Vis Sci.* 2016;57:5479–5489.
- Miller JML, Zhang Q, Johnson MW. Regression of drusen or vitelliform material heralding geographic atrophy: correlation between clinical observations and basic science. *Graefes Arch Clin Exp Ophthalmol.* 2021;259:2051–2053.
- Johnson LV, Forest DL, Banna CD, et al. Cell culture model that mimics drusen formation and triggers complement activation associated with age-related macular degeneration. *Proc Natl Acad Sci U S A.* 2011;108:18277–18282.
- Pilgrim MG, Lengyel I, Lanzirotti A, et al. Sub-retinal pigment epithelial deposition of drusen components including hydroxyapatite in a primary cell culture model. *Invest Ophthalmol Vis Sci.* 2017;58:708–719.
- Bretillon L, Thuret G, Gregoire S, et al. Lipid and fatty acid profile of the retina, retinal pigment epithelium/choroid, and the lacrimal gland, and associations with adipose tissue fatty acids in human subjects. *Exp Eye Res.* 2008;87:521–528.
- Wang L, Li C-M, Rudolf M, et al. Lipoprotein particles of intra-ocular origin in human Bruch membrane: an unusual lipid profile. *Invest Ophthalmol Vis Sci.* 2009;50:870–877.
- Harrison EH. Mechanisms of transport and delivery of vitamin A and carotenoids to the retinal pigment epithelium. *Mol Nutr Food Res.* 2019;63:e1801046.
- Vachali PP, Besch BM, Gonzalez-Fernandez F, Bernstein PS. Carotenoids as possible interphotoreceptor retinoid-binding protein (IRBP) ligands: a surface plasmon resonance (SPR) based study. *Arch Biochem Biophys.* 2013;539:181–186.

34. Hammond Jr BR, Wooten BR. CFF thresholds: relation to macular pigment optical density. *Ophthalmic Physiol Opt.* 2005;25:315–319.
35. Curcio CA, McGwin G, Sadda SR, et al. Functionally validated imaging endpoints in the Alabama Study on Early Age-Related Macular Degeneration 2 (ALSTAR2): design and methods. *BMC Ophthalmol.* 2020;20:96.
36. Davis MD, Gangnon RE, Lee LY, et al. The Age-Related Eye Disease Study severity scale for age-related macular degeneration: AREDS report no. 17. *Arch Ophthalmol.* 2005;123:1484–1498.
37. Craft NE. High resolution HPLC method for the simultaneous analysis of carotenoids, retinoids, and tocopherols. *FASEB J.* 1996;10:A27.
38. Craft NE. Chromatographic techniques for carotenoid separation. In: *Current Protocols in Food Analytical Chemistry*. Hoboken, NJ: John Wiley & Sons; 2001:F2.3.1–F2.3.15.
39. Delori FC. Autofluorescence method to measure macular pigment optical densities fluorometry and autofluorescence imaging. *Arch Biochem Biophys.* 2004;430:156–162.
40. Trieschmann M, Spital G, Lommatsch A, et al. Macular pigment: quantitative analysis on autofluorescence images. *Graefes Arch Clin Exp Ophthalmol.* 2003;241:1006–1012.
41. Berendschot TT, Goldbohm RA, Klopping WA, et al. Influence of lutein supplementation on macular pigment, assessed with two objective techniques. *Invest Ophthalmol Vis Sci.* 2000;41:3322–3326.
42. Schweitzer D, Jentsch S, Dawczynski J, et al. Simple and objective method for routine detection of the macular pigment xanthophyll. *J Biomed Opt.* 2010;15:061714.
43. Sauer L, Schweitzer D, Ramm L, et al. Impact of macular pigment on fundus autofluorescence lifetimes. *Invest Ophthalmol Vis Sci.* 2015;56:4668–4679.
44. Schindelin J, Arganda-Carreras I, Frise E, et al. Fiji: an open-source platform for biological-image analysis. *Nat Methods.* 2012;9:676–682.
45. Obana A, Gohto Y, Sasano H, et al. Grade of cataract and its influence on measurement of macular pigment optical density using autofluorescence imaging. *Invest Ophthalmol Vis Sci.* 2018;59:3011–3019.
46. Obana A, Ote K, Hashimoto F, et al. Correction for the influence of cataract on macular pigment measurement by autofluorescence technique using deep learning. *Transl Vis Sci Technol.* 2021;10:18.
47. Burke JD, Curran-Celentano J, Wenzel AJ. Diet and serum carotenoid concentrations affect macular pigment optical density in adults 45 years and older. *J Nutr.* 2005;135:1208–1214.
48. Hammond Jr BR, Curran-Celentano J, Judd S, et al. Sex differences in macular pigment optical density: relation to plasma carotenoid concentrations and dietary patterns. *Vis Res.* 1996;36:2001–2012.
49. Alassane S, Binquet C, Cottet V, et al. Relationships of macular pigment optical density with plasma lutein, zeaxanthin, and diet in an elderly population: the Montrachet study. *Invest Ophthalmol Vis Sci.* 2016;57:1160–1167.
50. Snodderly DM. Evidence for protection against age-related macular degeneration (AMD) by carotenoids and antioxidant vitamins. *Am J Clin Nutr.* 1995;62(Suppl):1448S–1461S.
51. Nolan JM, Stack J, O' Donovan O, et al. Risk factors for age-related maculopathy are associated with a relative lack of macular pigment. *Exp Eye Res.* 2007;84:61–74.
52. Koo E, Neuringer M, SanGiovanni JP. Macular xanthophylls, lipoprotein-related genes, and age-related macular degeneration. *Am J Clin Nutr.* 2014;100 Suppl 1:336S–346S.
53. Olvera-Barrios A, Kihara Y, Wu Y, et al. Foveal curvature and its associations in UK Biobank participants. *Invest Ophthalmol Vis Sci.* 2022;63:26.
54. Hendrickson AE, Yuodelis C. The morphological development of the human fovea. *Ophthalmology.* 1984;91:603–612.
55. Thomas MG, Papageorgiou E, Kuht HJ, Gottlob I. Normal and abnormal foveal development. *Br J Ophthalmol.* 2022;106:593–599.
56. Curcio CA, Sloan KR, Kalina RE, Hendrickson AE. Human photoreceptor topography. *J Comp Neurol.* 1990;292:497–523.
57. Ahmad KM, Klug K, Herr S, et al. Cell density ratios in a foveal patch in macaque retina. *Vis Neurosci.* 2003;20:189–209.
58. Hammond Jr BR, Wooten BR, Snodderly DM. Individual variations in the spatial profile of human macular pigment. *J Opt Soc Am A Opt Image Sci Vis.* 1997;14:1187–1196.
59. Delori FC, Goger DG, Keilhauer C, et al. Bimodal spatial distribution of macular pigment: evidence of a gender relationship. *J Opt Soc Am A Opt Image Sci Vis.* 2006;23:521–538.
60. Berendschot TT, van Norren D. Macular pigment shows ringlike structures. *Invest Ophthalmol Vis Sci.* 2006;47:709–714.
61. Kirby ML, Galea M, Loane E, et al. Foveal anatomic associations with the secondary peak and the slope of the macular pigment spatial profile. *Invest Ophthalmol Vis Sci.* 2009;50:1383–1391.
62. Obana A, Gohto Y, Sasano H, et al. Spatial distribution of macular pigment estimated by autofluorescence imaging in elderly Japanese individuals. *Jpn J Ophthalmol.* 2020;64:160–170.
63. Tariq A, Mahroo OA, Williams KM, et al. The heritability of the ring-like distribution of macular pigment assessed in a twin study. *Invest Ophthalmol Vis Sci.* 2014;55:2214–2219.
64. Zhang T, Godara P, Blanco ER, et al. Variability in human cone topography assessed by adaptive optics scanning laser ophthalmoscopy. *Am J Ophthalmol.* 2015;160:290–300.e1.
65. Pedersen HR, Neitz M, Gilson SJ, et al. The cone photoreceptor mosaic in aniridia: within-family phenotype-genotype discordance. *Ophthalmol Retina.* 2019;3:523–534.
66. Wynne N, Cava JA, Gaffney M, et al. Intergrader agreement of foveal cone topography measured using adaptive optics scanning light ophthalmoscopy. *Biomed Opt Express.* 2022;13:4445–4454.
67. Reiniger JL, Domdei N, Holz FG, Harmening WM. Human gaze is systematically offset from the center of cone topography. *Curr Biol.* 2021;31:4188–4193.e3.
68. Harrison EH, Curley Jr RW. Carotenoids and retinoids: nomenclature, chemistry, and analysis. *Subcell Biochem.* 2016;81:1–19.
69. Bohn T, Desmarchelier C, Dragsted LO, et al. Host-related factors explaining interindividual variability of carotenoid bioavailability and tissue concentrations in humans. *Mol Nutr Food Res.* 2017;61:1600685.
70. Bordoni L, Gabbianelli R. Primers on nutrigenetics and nutri(epi)genomics: origins and development of precision nutrition. *Biochimie.* 2019;160:156–171.
71. Liew SH, Gilbert CE, Spector TD, et al. Heritability of macular pigment: a twin study. *Invest Ophthalmol Vis Sci.* 2005;46:4430–4436.

72. Wang W, Connor SL, Johnson EJ, et al. Effect of dietary lutein and zeaxanthin on plasma carotenoids and their transport in lipoproteins in age-related macular degeneration. *Am J Clin Nutr*. 2007;85:762–769.
73. Zerbib J, Seddon JM, Richard F, et al. rs5888 variant of SCARB1 gene is a possible susceptibility factor for age-related macular degeneration. *PLoS One*. 2009;4:e7341.
74. McKay GJ, Loane E, Nolan JM, et al. Investigation of genetic variation in scavenger receptor class B, member 1 (SCARB1) and association with serum carotenoids. *Ophthalmology*. 2013;120:1632–1640.
75. Zheng W, Reem R, Omarova S, et al. Spatial distribution of the pathways of cholesterol homeostasis in human retina. *PLoS One*. 2012;7:e37926.
76. Li M, Jia C, Kazmierkiewicz KL, et al. Comprehensive analysis of gene expression in human retina and supporting tissues. *Hum Mol Genet*. 2014;23:4001–4014.
77. Tian Y, Kijlstra A, van der Veen RL, et al. The effect of lutein supplementation on blood plasma levels of complement factor D, C5a and C3d. *PLoS One*. 2013;8:e73387.
78. Tian Y, Kijlstra A, van der Veen RL, et al. Lutein supplementation leads to decreased soluble complement membrane attack complex sC5b-9 plasma levels. *Acta Ophthalmol*. 2015;93:141–145.
79. Kalariya NM, Ramana KV, Srivastava SK, van Kuijk FJ. Carotenoid derived aldehydes-induced oxidative stress causes apoptotic cell death in human retinal pigment epithelial cells. *Exp Eye Res*. 2008;86:70–80.
80. Chew EY, Clemons TE, Agron E, et al. Long-term outcomes of adding lutein/zeaxanthin and omega-3 fatty acids to the AREDS supplements on age-related macular degeneration progression: AREDS2 Report 28. *JAMA Ophthalmol*. 2022;140:692–698.
81. Thomas SE, Harrison EH. Mechanisms of selective delivery of xanthophylls to retinal pigment epithelial cells by human lipoproteins. *J Lipid Res*. 2016;57:1865–1878.
82. Pettersson T, Ernstrom U, Griffiths W, et al. Lutein associated with a transthyretin indicates carotenoid derivation and novel multiplicity of transthyretin ligands. *FEBS Lett*. 1995;365:23–26.
83. Bhosale P, Larson AJ, Frederick JM, et al. Identification and characterization of a pi isoform of glutathione S-transferase (GSTP1) as a zeaxanthin-binding protein in the macula of the human eye. *J Biol Chem*. 2004;279:49447–49454.
84. Li B, Vachali P, Frederick JM, Bernstein PS. Identification of StARD3 as a lutein-binding protein in the macula of the primate retina. *Biochemistry*. 2011;50:2541–2549.
85. Voigt AP, Mullin NK, Whitmore SS, et al. Human photoreceptor cells from different macular subregions have distinct transcriptional profiles. *Hum Mol Genet*. 2021;30:1543–1558.
86. Curcio CA, Johnson M, Huang J-D, Rudolf M. Apolipoprotein B-containing lipoproteins in retinal aging and age-related maculopathy. *J Lipid Res*. 2010;51:451–467.
87. Rodriguez IR, Clark ME, Lee JW, Curcio CA. 7-Ketocholesterol accumulates in ocular tissues as a consequence of aging and is present in high levels in drusen. *Exp Eye Res*. 2014;128:151–155.
88. Spaide R, Ho-Spaide W, Browne R, Armstrong D. Characterization of peroxidized lipids in Bruch's membrane. *Retina*. 1999;19:141–147.
89. Lee AY, Wu Y, Spaide T, et al. Exploring a structural basis for delayed rod-mediated dark adaptation in age-related macular degeneration via deep learning. *Transl Vis Sci Technol*. 2020;9:62.
90. Owsley C, Swain TA, McGwin Jr G, et al. How vision is impaired from aging to early and intermediate age-related macular degeneration: insights from ALSTAR2 baseline. *Transl Vis Sci Technol*. 2022;11:17.